Sensor and Simulation Notes

Note 519

Nov 2006

Comparison of Analytical and Numerical Results for a Prolate-Spheroidal Impulse-Radiating Antenna (IRA)

Serhat Altunc, Carl E. Baum and Christos G. Christodoulou

University of New Mexico
Department of Electrical and Computer Engineering
Albuquerque New Mexico 87131

Abstract

This paper deals with the numerical and analytical results for the focal waveform of a prolate-spheroidal IRA. Both numerical and analytical calculations are for IRAs with different feed arms. In both cases the comparisons between the numerical and analytical results are presented and discussed.

This work was sponsored in part by the Air Force Office of Scientific Research.

1. Introduction

While impulse-radiating antennas (IRAs) have been developed for the transient far field, in this paper we are going to focus in the near field for a biological application [1]. Numerical and analytical focal waveforms of a prolate-spheroidal IRA are calculated and compared. This paper is an extension of [2].

We use CST MICROWAVE STUDIO (CST MWS) for our numerical calculation. CST is a specialist tool for the 3D EM simulation of high frequency problems. CST is based on Finite Integration Technique (FIT). This numerical method provides a universal spatial discretization scheme, applicable to various electromagnetic problems, ranging from static field calculations to high frequency applications in time or frequency domain.

CST Applications include the expanding areas of: Mobile Communication, Wireless Design , Signal Integrity, and EMC. The broadly applicable Time Domain solver and the Frequency Domain solver simulates on hexahedral as well as on tetrahedral grids[5].

2. Description of geometry

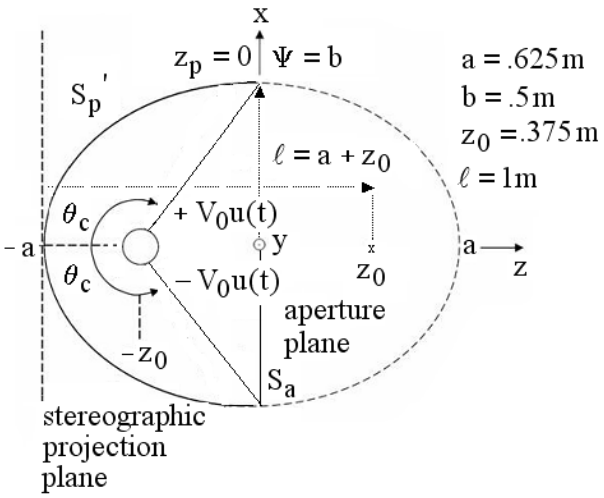

Figure 2.1 IRA Geometry

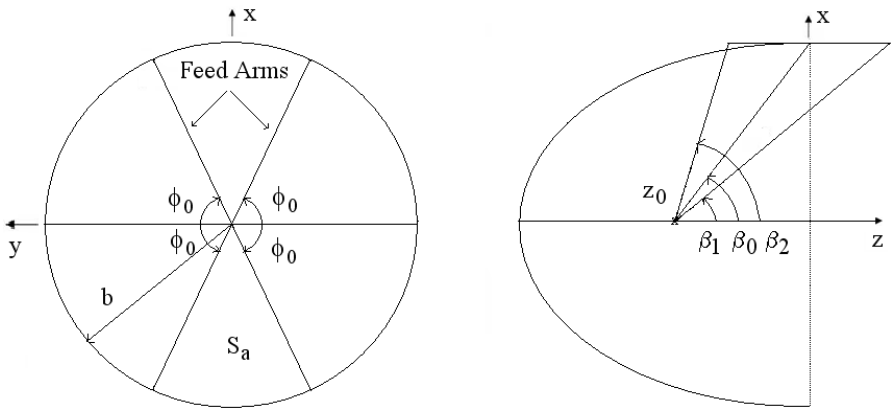

Figure 2.2 Feed Arm Geometry

We chose a special case of the prolate-spheroidal IRA's geometric parameters as [1]

$$z_p = 0,\ b = \Psi_0 = .5\,\text{m},\ a = .625\ \text{m},\ z_0 = .375\,\text{m},\ \ell = 1\,\text{m} \qquad (2.1)$$

For our later example calculations, our design has four TEM feed arms and the dimensions of these arms are determined by a $200\,\Omega$ pulse impedance ($\phi_0 = 45^o$, 60^o).

The feed-arm parameters, b_0, b_1, b_2, have been previously calculated in the stereographic projection plane for $\phi_0 = 60^o$ [3] as

$$b_0^{\,2} = b_1 b_2 \ \ , \ \ (b_1 - b_2)/b_0 = 0.521 \qquad (2.2)$$

from which we find the angles for the four-feed arms as

$$\beta_0 = \arctan(.5/.375) \cong 53.1^o \ , \ \beta_1 = 2\arctan\left[\sqrt{b_1/b_2}\,\tan(\beta_0/2)\right] = 42.23^o$$
$$\beta_2 = 2\arctan\left[\sqrt{b_1/b_2}\,\tan(\beta_1/2)\right] = 65.77^o \qquad (2.3)$$

β_0 , β_1 , β_2 are the angles from the z-axis to the electrical center, first edge and second edge.

From (2.2), (2.3) and table 1 [3], we can find the locations and dimensions of the feed arms. The feed arms are symmetric and the upper fed arms have three corners located at

Right			Left		
x_1	y_1	z_1	x_2	y_2	z_2
0	0	-37.5	0	0	-37.5
43.3	25	-15	43.3	-25	-15
43.3	25	18	43.3	-25	18

Table 2.1 Upper feed arms corner locations in cm for 60^o 4-TEM-Feed-Arm

In this paper, we concentrate on three different types of feed-arm geometry based on the choice of ϕ_0, the feed arm angle. The first feed design has two 90^o TEM feed arms and the dimensions of these arms are determined by a $400\,\Omega$ pulse impedance. The second and third designs use 45^o and 60^o TEM feed arms and the dimensions of these arms are determined by $200\,\Omega$ pulse impedance. The 45^o case has the same dimensions as the two-arm case, by symmetry.

Farr introduced the voltage normalized gain as $G_v = h_a / f_g$ [4,5], and this can be used for comparison to the radiation from two different antennas that have the same input voltage. Here h_a is the aperture height and $f_g = Z_c / Z_0$ is the impedance factor which relates the transmission-line impedance to the free space impedance. From table 1 of [3] we can easily define

$$G_{v1} = \frac{.736}{200/377} = 1.387 \ , \ G_{v2} = \frac{.648}{200/377} = 1.221 \qquad (2.4)$$

G_{v1} and G_{v2} are the voltage gain for four 60^o and 45^o (times .707 for the two-arm, $400\,\Omega$, case by symmetry) TEM-feed-arms case. If we divide G_{v1} by G_{v2}, we can determine the increase in the field if we use the 60^o instead of 45^o. So we have $G_{v1}/G_{v2} = 1.135$. We know that we will have a $\sqrt{2}$ increase in the field values if we have a four 45^o TEM feed arms instead of 2 arms, due to symmetry. So we should have, a $\left[G_{v1}/G_{v2}\right]\sqrt{2} = 1.606$, increase in the fields with using the 60^o TEM-feed-arm case as compared with the 2-arm case. In our design we used the 60^o because the voltage gain is nearly maximum [3].

3. Numerical Focal Waveforms for 2-TEM-Feed-Arm Case

For all numerical calculations the number of lines per wavelength is 8. the frequency is either 3 or 5 GHz. An accurate analytical result for 2-TEM-feed-arm case is [4]

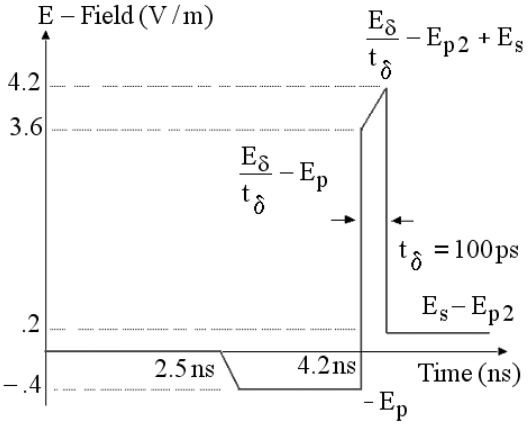

Figure 3 Analytic Waveform at the Second Focus for 2-TEM-feed-arm case

3.1 Numerical focal waveforms for 3GHz vs 5 GHz

Calculated simulation results for 3 GHz and 5 GHz

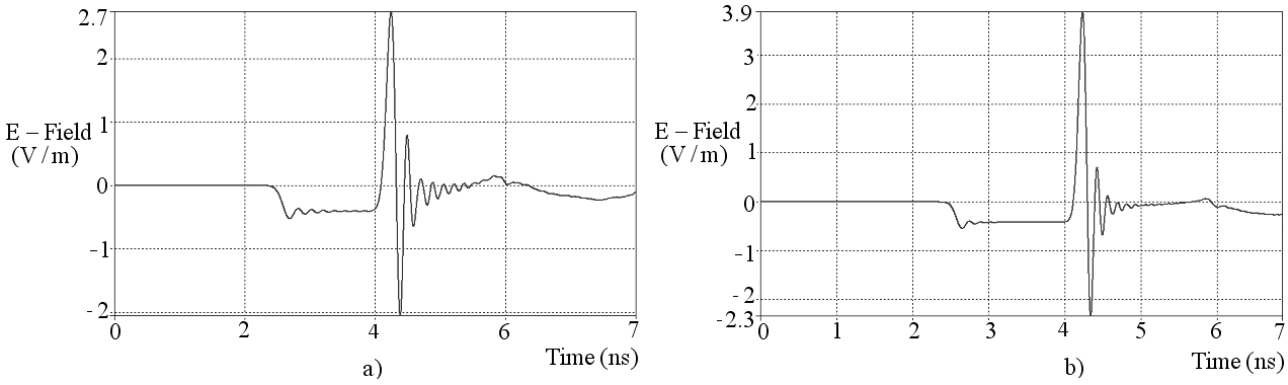

Figure 3.1 Numerical Waveform at the Second Focus at a) 3 GHz b) 5 GHz

One can see that from Fig. 3.1 if we use 5 GHz instead of 3 GHz we obtain a closer result (to the analytical result) for the pulse peak.

3.2 Numerical focal waveform with smoother rise for excitation

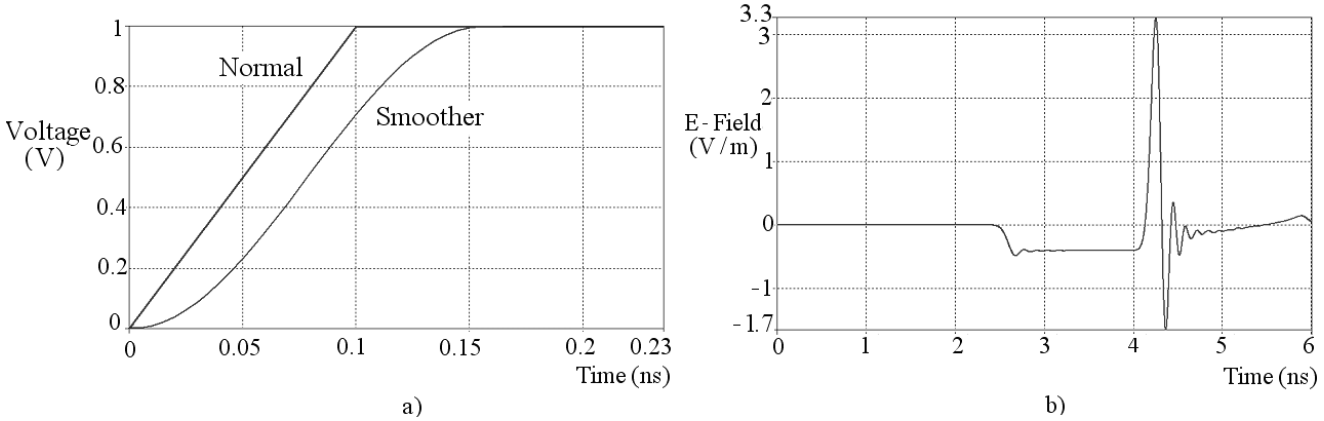

Figure 3.2 a) Normal and Smoother Excitation b)Waveform for Smoother Excitation at 5GHz

We did this to have the same t_{mr} (based on maximum rate of rise). For a step like $f(t)$

$$t_{mr} = \frac{f_{max}}{\left.\frac{df}{dt}\right|_{max}} \tag{3.1}$$

we have same t_{mr} but no discontinuities in slope (derivative) to reduce the required high frequencies. We can see that peak is not as high as for the normal excitation but there is significantly less late-time oscillation amplitude.

3.3 Numerical focal waveform for 200ps risetime instead of 100ps

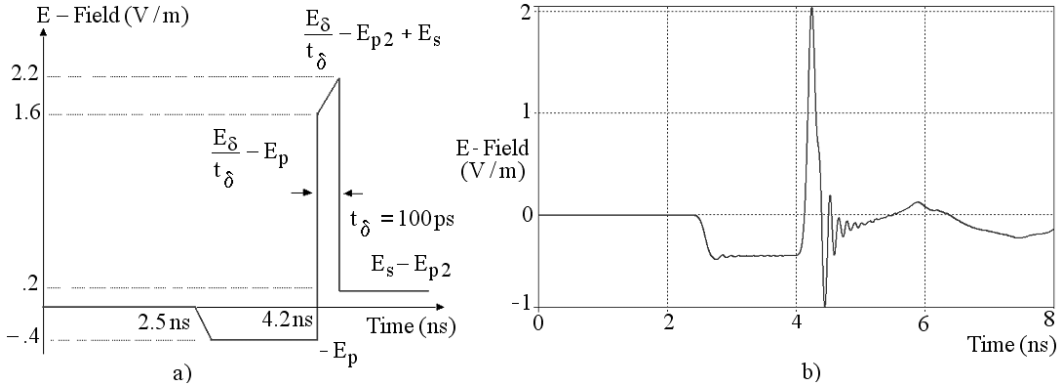

Figure 3.3 Focal waveform for 200ps risetime instead of 100ps for 5 GHz
a) Analytical b) Numerical

One can see that from Fig. 3.3 by reducing risetime, we need less high frequencies, so we obtain closer agreement with the analytical results for the impulse peak.

4. Numerical and Analytical Focal Waveforms for Different Feed Arms for 5 GHz Upper Frequency

4.1 2-Arm, 90^{o}, 400Ω Numerical vs Analytical Results

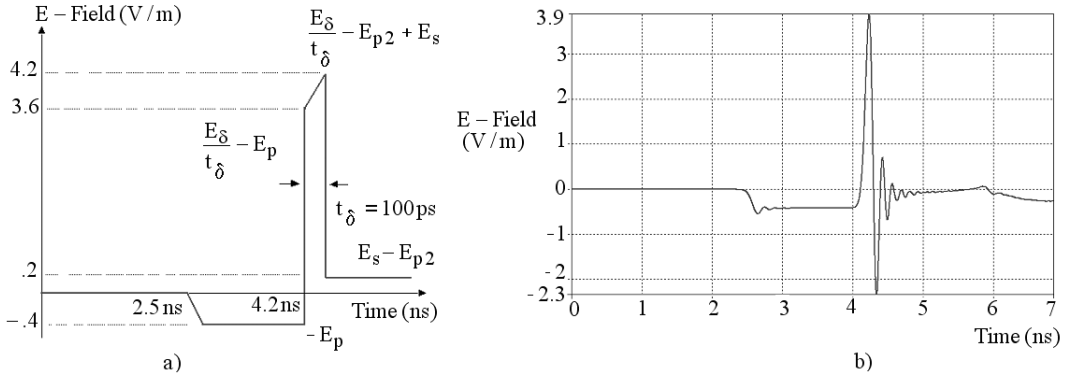

Figure 4.1 Waveform for 90^{o} 2-TEM-Feed-Arm Case a) Analytical b)Numerical

4.2 4 Arms, 45^{o}, 200Ω Numerical vs Analytical Results

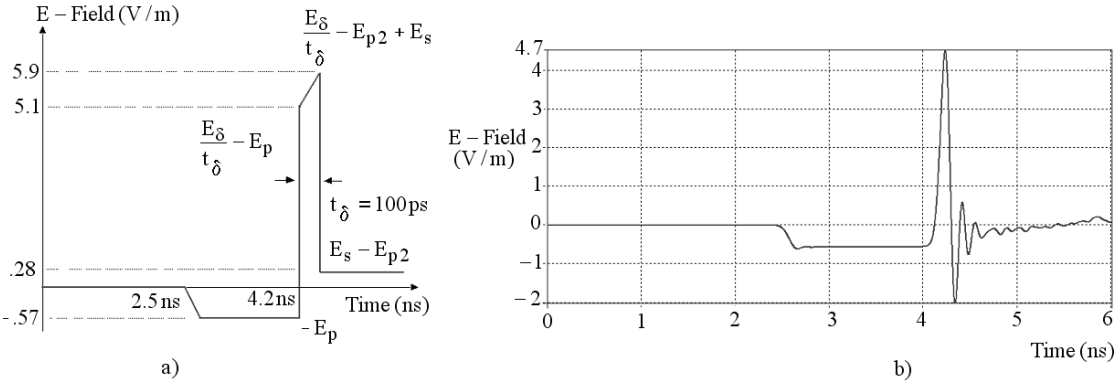

Figure 4.2 Waveform for 45^{o} 4-TEM-Feed-Arm Case a) Analytical b)Numerical

4.3 4 Arms, 60^{o}, 200Ω Numerical vs Analytical Results

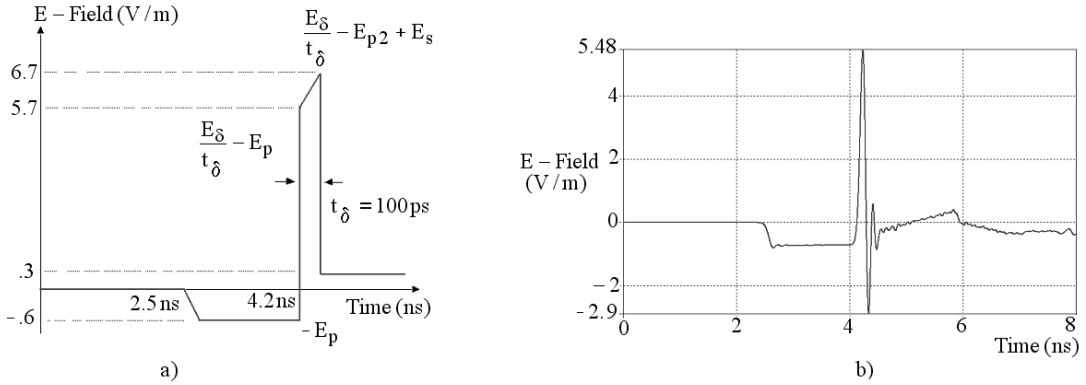

Figure 4.3 Waveform for 60^{o} 4-TEM-Feed-Arm Case a) Analytical b) Numerical

The excitation is a 1 Volt ($V_0 = .5$ Volt) step, rising as a ramp function lasting 100 ps.. The numerical calculations have errors. There are errors in the numerical technique(e.g., spatial dispersion). The prepulse is rather good. The impulse is trying to approach the analytical shape and value, but the postpulse has no relation to the physical case. Finally, there is also the plane-wave approximation on S_a for calculating G_v numerically. The wave is spherical, introducing some errors. G_v is calculated in [5-7] for a planar wave. It may be a little different for a spherical wave when accounting for the plate widths. This would require more detailed calculations.

4.Conclusion

For the 2-arm and 4-arm-45^0 cases the prepulse of –0.4 agrees very closely between the analytical and numerical cases. For the 4-arm-60^o case the analytic prepulse is -0.6 while the numerical case is -0.7 (some error). The impulse part shows less agreement, between analytical and numerical, approaching the analytical value from below, likely due to the high-frequencies required. Analytical errors can be classified into two groups. First of all, analytical calculation does not account for feed arm width, and it is a little different from [7]. Secondly, when calculating the aperture integrals we have used the uniform-field part all the way to $\Psi = \Psi_p$ but the feed arms intersect partly into S_a for $\Psi < \Psi_p$. So the aperture integrals are correct up to some radius less than Ψ_p. Note that 60^0 arms are much wider than 45^0 arms for the same $200\,\Omega$ impedance. The analytical waveform, while simple, is still good, but not perfect.

We are expecting to get more reasonable results with our experiments.

References

1. K. H. Schoenbach, R. Nuccitelli and Stephen J. Beebe, “ZAP”, IEEE Spectrum, Aug 2006, Pg 20-26.
2. C. E. Baum, “Focal Waveform of a Prolate-Spheroidal IRA”, Sensor and Simulation Note 509, February 2006.
3. M. J. Baretela and J. S. Tyo, “Improvement of prompt radiated response from impulse radiating antennas by aperture trimming,” *IEEE Trans. Antennas Propagat.*, vol. 51, pp. 2158 – 2167, 2003.
4. S.Altunc and C.E.Baum. “Extension of the Analytic Results for the Focal Waveform of a Two-Arm Prolate-Spheroidal Impulse-Radiating Antenna (IRA)”, Sensor and Simulation Note 518, Nov 2006.
5. E. G. Farr, “Optimizing the feed impedance of impulse radiating antennas. Part I. Reflector IRAs,” in *Sensor and Simulation Notes #354*,C. E. Baum, Ed. Abq, NM: Phillips Laboratory, 1993.
6. E. G. Farr and C. E. Baum, “Impulse radiating antennas III,” in *Ultra-Wideband, Short-Pulse Electromagnetics 3*, C. E. Baum, L. Carin, and P. Stone, Eds. New York: Plenum, 1997, pp. 43–56.
7. C.E. Baum, “Radiation of Impulse-Like Transient Fields”, Sensor and Simulation Note 321, Nov 1998.